Theor Appl Climatol (2011) 105:357–370
DOI 10.1007/s00704-010-0388-2

ORIGINAL PAPER

Comparison of human radiation exchange models in outdoor areas

Sookuk Park · Stanton E. Tuller

Received: 1 June 2010 / Accepted: 10 December 2010 / Published online: 11 January 2011

Abstract Results from the radiation components of seven different human thermal exchange models/methods are compared. These include the Burt, COMFA, MENEX, OUT_SET* and RayMan models, the six-directional method and the new Park and Tuller model employing projected area factors (f_p) and effective radiation area factors (f_{eff}) determined from a sample of normal- and over-weight Canadian Caucasian adults. Input data include solar and longwave radiation measured during a clear summer day in southern Ontario. Variations between models came from differences in f_p and f_{eff} and different estimates of longwave radiation from the open sky. The ranges between models for absorbed solar, net longwave and net all-wave radiation were 164, 31 and 187 Wm^{-2}, respectively. These differentials between models can be significant in total human thermal exchange. Therefore, proper f_p and f_{eff} values should be used to make accurate estimation of radiation on the human body surface.

Symbols

a_b	Albedo (reflectivity) of a person's body surface (0.3)
a_o	Mean albedo of ground-based, solid objects projecting into the sky hemisphere (0.2)
a_g	Albedo of ground (0.3)
A_{eff}	Effective radiation area (square metres)
A_D	Total body surface area (square metres)
A_P	Projected body surface area (square metres)
e_a	Air vapour pressure (hectopascals)
f_{eff}	Effective radiation area factor ($=A_{eff}/A_D$)
f_p	Projected area factor per unit of effective radiation body area ($=A_p/A_{eff}$)
f_p^*	Projected area factor per unit of total body area ($=A_p/A_D=f_p\times f_{eff}$)
K_b	Incoming direct beam solar radiation on a horizontal surface (watts per square metre)
K_b^*	Absorbed direct beam solar radiation on the body surface (watts per square metre)
K_d	Diffuse beam solar radiation from the sky on the horizontal ground surface (watts per square metre)
K_d^*	Diffuse beam solar radiation from the sky absorbed on the body surface (watts per square metre)
K_r	Total reflected solar radiation by objects and ground ($=K_{ro}+K_{rg}$) (watts per square metre)
K_r^*	Total solar radiation reflected by objects and ground absorbed on the body surface (watts per square metre)
K_{rg}	Solar radiation reflected by the ground (watts per square metre)
K_{ro}	Solar radiation reflected by objects in the sky hemisphere (buildings, trees and other structures) (watts per square metre)
L	Net longwave radiation on the body surface (watts per square metre)
L_a	Incoming longwave radiation from the sky to the horizontal ground surface (watts per square metre)
L_b	Longwave radiation emitted from the body surface (watts per square metre)

S. Park (✉) · S. E. Tuller
Climate Laboratory, Department of Geography,
University of Victoria,
P.O. Box 3060, Stn CSC,
Victoria, BC, Canada V8W 3R4
e-mail: sooland@uvic.ca

S. Park
e-mail: sooland@gmail.com

L_g Longwave radiation emitted from the ground (watts per square metre)
L_o Longwave radiation coming from objects in the sky hemisphere to the horizontal ground surface (watts per square metre)
Q Net all-wave radiation on the body surface (watts per square metre)
R Absorbed solar (shortwave) radiation on the body surface (watts per square metre)
RH Relative humidity (decimal)
t Transmissivity for direct beam solar radiation of objects obscuring the sun [building=0, trees vary from 0.15 (spruce) to 0.75 (willow), from Brown and Gillespie (1995)]
T_a Air temperature (degrees Celsius)
T_b Skin temperature (degrees Celsius)
Z_{sl} The angle between the perpendicular to the object surface and the sun (degrees)
ψ_{sky} Sky view factor (decimal)
ψ_{w_sky} The view factor of sky seen from the object surface (decimal)
β (Solar) altitude angle (degrees)
ε_a Emissivity of air (0.97 to 0.99)
ε_b Emissivity of the body surface (0.97)
ε_{sky} Sky emissivity
σ Stefan–Boltzmann constant ($5.67 \cdot 10^{-8}$ W m^{-2} K^{-4})

1 Introduction

A number of human thermal exchange models have been developed which include all important modes of energy exchange. Some of those capable of use in outdoor urban environments are the Burt model (Burt 1979 and modified by Tuller 1990), COMFA (COMfort FormulA; Brown and Gillespie 1986, 1995), MENEX (Man-ENvironment heat Exchange; Blazejczyk 1994, 2004, 2005), RayMan (Matzarakis et al. 2000, 2007, 2009) and OUT-SET* (Pickup and de Dear 2000).

Urban outdoor environments have a very important and different climatic variable, solar radiation, compared with indoor environments. Solar radiation can raise the apparent temperature between 7°C and 14°C depending on wind speed (Steadman 1971).

Early versions of different methods for estimating solar radiation absorbed on the human body surface were reviewed by Blazejczyk et al. (1993) using Krys and Brown's (1990) cylindrical body type equation which is a solar radiation component of the COMFA model. Park and Tuller (2010) analysed human body area factors (effective radiation area and projected area factors) for standing and walking postures and compared these with previous studies, e.g. Underwood and Ward (1966), Fanger (1972), Tanabe et al. (2000) and Kubaha et al. (2004) for standing posture; Ward and Underwood (1967) and Steadman (1979) for walking posture.

Four different approaches have been used to analyse the effects of human body shape on human solar and longwave radiation exchange. The first is experimental results from a photographic method such as used in the Park and Tuller and RayMan models. The second is also experimental results from a standing person's shadow patterns on the ground surface used in the Burt model or a mannequin as an analogue model of the human body used in the MENEX model. The third assumes the human body is a cylinder used in the COMFA and OUT_SET* models (Kenny et al. 2008; Spagnolo and de Dear 2003). The COMFA model uses a directionless cylinder, and the OUT_SET* model uses Underwood and Ward's (1966) elliptical cylinder (major axis facing the sun). The last is a cube combined with six-direction measured radiation data (upward, downward, east, west, south and north) (VDI 1998; Huang et al. 2005; Ali-Toudert et al. 2005; Matzarakis et al. 2007; Oliveira and Andrade 2007; Thorsson et al. 2007). Huang et al. (2005) used weighting factors of 0.238 for each of the four cardinal directions and 0.024 for up- and downward. Other researchers adopted the weighting factors from VDI (1998): 0.22 for each cardinal direction and 0.06 for up- and downward based on the directionless mean projected area factors of Fanger (1972).

The four different concepts of the human body shape can create large differences among models in the body area factors used in radiation analysis. The important body area factors are the effective radiation area factor (f_{eff}) and projected area factor (f_p). Body shape and posture control the area exposed to direct beam solar radiation (projected area, A_p) and the total body surface area exposed to the surrounding radiant environment rather than to other body parts (effective radiation area, A_{eff}). f_p ($=A_p/A_{eff}$) and f_p^* ($=A_p/A_D=f_p \times f_{eff}$, where A_D is the total body surface area) are used in the calculation of direct beam solar radiation. f_p is used in a formula for calculating the mean radiant temperature (T_{mrt}) in predicted mean vote (PMV, Fanger 1972) and RayMan, and f_p^* is used in the Burt, COMFA, MENEX and OUT_SET* models. f_{eff} ($=A_{eff}/A_D$) is employed to estimate all solar and longwave exchanges.

In this study, results from the radiation components of five existing human thermal exchange models (Burt, COMFA, MENEX, OUT_SET* and RayMan models) along with the six-directional method (VDI 1998) and a new human radiation exchange model, Park and Tuller model, are compared. The latter model employs mean body area factors (f_{eff} and f_p) of standing and walking postures determined from a sample of 139 normal- and over-weight Caucasian adults (Park and Tuller 2010).

Emphasis is on the effect of differences in human body area factors.

2 Materials and methods

2.1 Radiation models

Net all-wave radiation on the human body surface (Q) is the sum of absorbed total solar (shortwave) radiation (R) and net longwave (terrestrial) radiation (L) on the surface:

$$\pm Q = R \pm L \text{ (watts per square metre)} \quad (1)$$

2.1.1 Absorbed solar radiation

The units of all radiation streams and used in all models in this study are watts per square metre.

Park and Tuller model

$$\begin{aligned} R &= K_b^* + K_d^* + K_r^* \\ &= \left\{ f_p \cdot f_{eff} \cdot \frac{K_b}{\sin\beta} t + \frac{1}{2} f_{eff} \left[K_d \cdot \psi_{sky} + \left(K_b \cdot \cos Z_{sl} \cdot t + K_d \cdot \psi_{w\_sky} \right) a_o + \left(K_b \cdot t + K_d \cdot \psi_{sky} + K_{ro} \right) a_g \right] \right\} (1 - a_b) \\ &= \left\{ f_p^* \frac{K_b}{\sin\beta} t + \frac{1}{2} f_{eff} \left[K_d \cdot \psi_{sky} + K_{ro} + K_{rg} \right] \right\} (1 - a_b) \end{aligned} \quad (2)$$

f_p^* is $f_p \times f_{eff}$. f_p can be calculated with a formula, $f_p = 3.34 \cdot 10^{-7}\beta^3 - 6.60 \cdot 10^{-5}\beta^2 + 8.42 \cdot 10^{-4}\beta + 0.297$, from Park and Tuller (2010) for the mean of directionless standing and walking postures. The formula yields f_p within 0.002 of measured f_p values. t is transmissivity of objects for direct beam solar radiation between the specific object of interest and the sun. Z_{sl} is the angle between the perpendicular to the object surface and the sun. ψ_{w_sky} is the view factor of open sky seen from the object surface. The mean value of f_{eff} for standing and walking postures from the sample of Caucasian male and female adults in Canada, 0.836, was used in this model (Park and Tuller 2010).

RayMan model The equation is assumed to be same as the Park and Tuller model's except for values of f_p and f_{eff}. f_p can be calculated with the formula, $f_p = 0.308 \cos\left[\beta\left(0.998 - \beta^2/50000\right)\right]$ (Jendritzky et al. 1990), which was derived from Fanger's (1972) directionless f_p values for standing posture. The formula results are within 0.004 of Fanger's (1972) measured data. Fanger's f_{eff} result for standing posture, 0.725, is used in this model (Matzarakis et al. 2009).

MENEX model

$$R = \left[f_p^* \cdot K_b + (K_d + K_r)(0.0018 + 0.0462 \ln\beta) \right] (1 - a_b) \quad (3)$$

This model does not use an f_{eff}. f_p^* can be calculated from:

$$\begin{aligned} &\text{if } \beta \le 5^\circ, f_p^* = 1.4e^{(-0.51 + 0.368\beta)} \\ &\text{if } \beta > 5^\circ, f_p^* = \frac{26.34}{\beta} - 0.329 \end{aligned} \quad (4)$$

OUT_SET model*

$$R = \left\{ f_p^* \frac{K_b}{\sin\beta} + f_{eff} \left[K_d + (K_b + K_d) a_g \right] \right\} (1 - a_b) \quad (5)$$

f_p^* can be estimated from an equation of Underwood and Ward's (1966) elliptical cylinder model (orientation: major axis facing the sun):

$$f_p^* = (0.42 \cos\beta + 0.043 \sin\beta) \quad (6)$$

f_{eff} is 0.75 (Jendritzky and Nübler 1981). This model does not have the ½ function in estimating the K_d and K_r components. The ½ function accounts for the fact that a unit area of the vertical body surface is exposed to only ½ of the upper and lower hemispheres. Therefore, the unit area receives only ½ of the measured diffuse beam and reflected radiation on/from a horizontal surface.

Burt model

$$R = \left\{ f_p^* \cdot K_b + \frac{1}{2} f_{eff} \left[K_d + (K_b + K_d) a_g \right] \right\} (1 - a_b) \quad (7)$$

f_{eff} is 0.725 from Fanger (1972). The f_p^* equation is originally from Terjung and Louie (1971):

$$f_p^* = 4.278 \exp(-0.0512\beta) \quad (8)$$

COMFA model

$$R = \left\{ f_p^* \cdot K_b \cdot t + \frac{1}{2} f_{eff} \left[K_d + \left(K_b \cdot \cos Z_{sl} \cdot t + K_d \cdot \psi_{w\_sky} \right) a_o + \left(K_b \cdot t + K_d \cdot \psi_{sky} + K_{ro} \right) a_g \right] \right\} (1 - a_b) \quad (9)$$

This model did not originally use half the quantity of diffuse and reflected solar radiation. This was included by Kenny et al. (2008). f_{eff} is 0.78 for medium body build erect (standing) posture from Kerslake (1972) (originally from Guibert and Taylor 1952). f_p^* is estimated from a formula:

$$f_p^* = \frac{1/\tan\beta}{\pi} \quad (10)$$

2.1.2 Net longwave radiation

All models except the COMFA and Park and Tuller models assume an unobstructed upper (sky) hemisphere, which means ψ_{sky} is 1.0 (100%). Therefore, there is no longwave radiation emitted from vertical obstructions such as building and tree components (L_o). All models were modified to include this term by incorporating the components of ψ_{sky} and $1-\psi_{sky}$ in the model comparison.

Park and Tuller model

$$\begin{aligned} L &= \frac{1}{2} f_{eff} \cdot \varepsilon_b \left[\varepsilon_{sky} \cdot \sigma (T_a + 273)^4 \psi_{sky} + \varepsilon_o \cdot \sigma (T_o + 273)^4 \left(1 - \psi_{sky} \right) + \varepsilon_g \cdot \sigma \left(T_g + 273 \right)^4 \right] - f_{eff} \cdot \varepsilon_b \cdot \sigma (T_b + 273)^4 \\ &= \frac{1}{2} f_{eff} \cdot \varepsilon_b \left(L_a + L_o + L_g \right) - f_{eff} \cdot L_b \end{aligned} \quad (11)$$

f_{eff} is 0.836.

MENEX model

$$\begin{aligned} L &= \frac{1}{2} \varepsilon_b \left[\varepsilon_a \cdot \sigma (T_a + 273)^4 \left(0.82 - 0.25 \cdot 10^{-0.094 e_a} \right) \psi_{sky} + \varepsilon_o \cdot \sigma (T_o + 273)^4 \left(1 - \psi_{sky} \right) + \varepsilon_g \cdot \sigma \left(T_g + 273 \right)^4 \right] - \varepsilon_b \cdot \sigma (T_b + 273)^4 \\ &= \frac{1}{2} \varepsilon_b \left[\varepsilon_a \cdot \sigma (T_a + 273)^4 \left(0.82 - 0.25 \cdot 10^{-0.094 e_a} \right) \psi_{sky} + L_o + L_g \right] - L_b \end{aligned} \quad (12)$$

$$e_a = RH \times \exp\left(18.956 - \frac{4030.18}{T_a + 235} \right) \quad (13)$$

This model adopted the equation of sky emissivity $\left[\varepsilon_{sky} = \varepsilon_a \left(0.82 - 0.25 \cdot 10^{-0.094 e_a} \right) \right]$ from Geiger (1965). e_a is calculated with Antoine's equation (Parsons 1993). This model does not use an f_{eff}. 0.97 is used for ε_a.

RayMan model This model uses the same Geiger (1965) sky emissivity equation as the MENEX model (Matzarakis et al. 2009). However, to facilitate the comparison of the effects of Fanger's (1972) f_{eff} value with those used in other models, the longwave radiation formula applied in this paper is assumed to be the same as Park and Tuller's except the value of f_{eff}, 0.725.

OUT_SET model*

$$\begin{aligned} L &= \frac{1}{2} f_{eff} \cdot \varepsilon_b \left\{ \sigma \left[0.7 + 5.95 \cdot 10^{-5} e_a \exp\left(\frac{1500}{T_a + 273} \right) \right] (T_a + 273)^4 \psi_{sky} + \varepsilon_o \cdot \sigma (T_o + 273)^4 \left(1 - \psi_{sky} \right) + \varepsilon_g \cdot \sigma \left(T_g + 273 \right)^4 \right\} - f_{eff} \cdot \varepsilon_b \cdot \sigma (T_b + 273)^4 \\ &= \frac{1}{2} f_{eff} \cdot \varepsilon_b \left\{ \sigma \left[0.7 + 5.95 \cdot 10^{-5} e_a \exp\left(\frac{1500}{T_a + 273} \right) \right] (T_a + 273)^4 \psi_{sky} + L_o + L_g \right\} - f_{eff} \cdot L_b \end{aligned} \quad (14)$$

The equation for calculating sky emissivity $\left[\varepsilon_{sky} = 0.7 + 5.95 \cdot 10^{-5} e_a \exp\left(\frac{1500}{T_a+273}\right)\right]$ is from Idso (1981). f_{eff} is 0.75.

Burt model

$$L = \frac{1}{2} f_{eff} \cdot \varepsilon_b \left[\varepsilon_a \cdot \sigma (T_a + 273)^4 \left(0.55 + 0.065 {e_a}^{1/2}\right) \psi_{sky} + \varepsilon_o \cdot \sigma (T_o + 273)^4 \left(1 - \psi_{sky}\right) + \varepsilon_g \cdot \sigma \left(T_g + 273\right)^4\right] - f_{eff} \cdot \varepsilon_b \cdot \sigma (T_b + 273)^4$$
$$= \frac{1}{2} f_{eff} \cdot \varepsilon_b \left[\varepsilon_a \cdot \sigma (T_a + 273)^4 \left(0.55 + 0.065 {e_a}^{1/2}\right) \psi_{sky} + L_o + L_g\right] - f_{eff} \cdot L_b \quad (15)$$

The equation for calculating sky emissivity $\left[\varepsilon_{sky} = \varepsilon_a \left(0.55 + 0.065 {e_a}^{1/2}\right)\right]$ is originally from Brunt (1932) and evaluated by Iziomon et al. (2003) converting the units of e_a from millimetres of mercury to hectopascals. f_{eff} is 0.725. ε_a in this model is 0.99.

COMFA model

$$L = \frac{1}{2} f_{eff} \cdot \varepsilon_b \left\{\left[1.2\varepsilon_a \cdot \sigma (T_a + 273)^4 - 171\right] \psi_{sky} + \varepsilon_o \cdot \sigma (T_o + 273)^4 \left(1 - \psi_{sky}\right) + \varepsilon_g \cdot \sigma \left(T_g + 273\right)^4\right\} - f_{eff} \cdot \varepsilon_b \cdot \sigma (T_b + 273)^4$$
$$= \frac{1}{2} f_{eff} \cdot \varepsilon_b \left\{\left[1.2\varepsilon_a \cdot \sigma (T_a + 273)^4 - 171\right] \psi_{sky} + L_o + L_g\right\} - f_{eff} \cdot L_b \quad (16)$$

The regression equation for estimating longwave radiation from the clear sky as a function of air temperature is from Swinbank (1963). f_{eff} is 0.78. ε_a is 0.98.

2.2 Radiation data

To compare the existing radiation models, clear summer data collected three times on August 10, 2002 were used: in the morning (0730–0900 hours), around noon (1130–1300 hours) and in the afternoon (1530–1700 hours). The research site was Winegard Walk at the University of Guelph, Guelph, Ontario, Canada (Fig. 1). The latitude and longitude of the site are N43°32′, W80°14′. The mean ground elevation is 345 m above sea level. For this study, only the data observed at sunny locations were used as reference data for the radiation analysis: 4 locations (no. 1, 8, 9, 11) in the morning, all 13 locations around noon and 8 locations (no. 1, 3, 5, 8, 9, 10, 11, 13) in the afternoon (Fig. 2 and Table 1).

A Kipp & Zonen CNR1 net radiometer was used to collect both shortwave and longwave radiation. This instrument has two CM 3 pyranometers and two CG 3 pyrgeometers, one of each mounted to face in opposite directions (e.g. up- and downward). Each pyranometer has a 180° field of view, and both of them will cover the entire sphere. Each pyrgeometer's field of view is only 150°, so both of them will cover 300° not the entire sphere. However, the differences of collected longwave radiation that can be created by the short field of view are negligible, e.g. 5.4 Wm^{-2} when total incoming longwave radiation from an entire hemisphere is 400 Wm^{-2} if the entire hemisphere is assumed as an isothermal environment. Radiation data were collected from six directions (up- and downward and the four cardinal directions) for 1 min for each two directions at the height of 1.2 m and saved every 5 s on a 21x datalogger, made by Campbell Scientific Corporation. To collect air temperature, a Mannix Model CMM880 digital thermo-hygrometer was used. Humidity data were measured at the nearby Guelph Turfgrass Institute. For more detail, see Park (2003).

To simply compare the models, the effect of clothing was not included in the calculation. The albedoes of the body surface (a_b), objects in the sky hemisphere (a_o) and ground (a_g) and emissivity of the body surface (ε_b) were set to 0.3, 0.2, 0.3 and 0.97, respectively. These values were frequently used in previous modelling studies. The same values of incoming direct beam (K_b), diffuse beam (K_d), reflected (K_r) by objects (buildings, trees and other structures) in the sky hemisphere (K_{ro}) and by the ground (K_{rg}) solar radiation, and longwave radiation coming from objects in the sky hemisphere (L_o) and ground (L_g) derived from the measured data were directly used in all radiation models (Table 1 and Fig. 2). The Park and Tuller, RayMan and six-directional models employed measured longwave radiation from the sky (L_a). L_a values computed from air temperature and humidity via Eqs. 14 through 18 were used in the other four models. Gagge et al. (1969) found that human skin temperature (T_b) was between 27°C and 36.5°C in steady-state conditions. Within this range of T_b, the

Fig. 1 The view of Winegard Walk and the 13 observation locations

greatest difference in longwave radiation emitted by the body surface (L_b) between the greatest and lowest f_{eff} compared in this study, 0.836 from the Park and Tuller model and 0.725 from Fanger (1972), was only 6 Wm^{-2}. Thus, a T_b of 31°C was assumed for all simulations.

The amounts of solar and longwave radiation mentioned above were calculated from radiation data collected on a horizontal surface. They were not the quantities of radiation on a body surface perpendicular to the sun's rays. The Burt and COMFA models used f_p^* values developed on the basic concept of shadow areas of a standing person on the horizontal ground surface (Terjung and Louie 1971, Fig. 3a). In contrast, the OUT_SET*, RayMan and Park and Tuller models took the perpendicular to the sun's rays surface area concept (Fig. 3b). The perpendicular concept models should be multiplied by $1/\cos(90-\beta)=1/\sin\beta$ to facilitate direct application of direct beam solar radiation measured on a horizontal surface. β is solar altitude (elevation).

All models except the Park and Tuller and COMFA models are for unobstructed horizons. They do not have components for the open sky view factor (ψ_{sky}) and reflected solar radiation from objects in the sky hemisphere (K_{ro}). Therefore, fixed values of diffuse and reflected solar

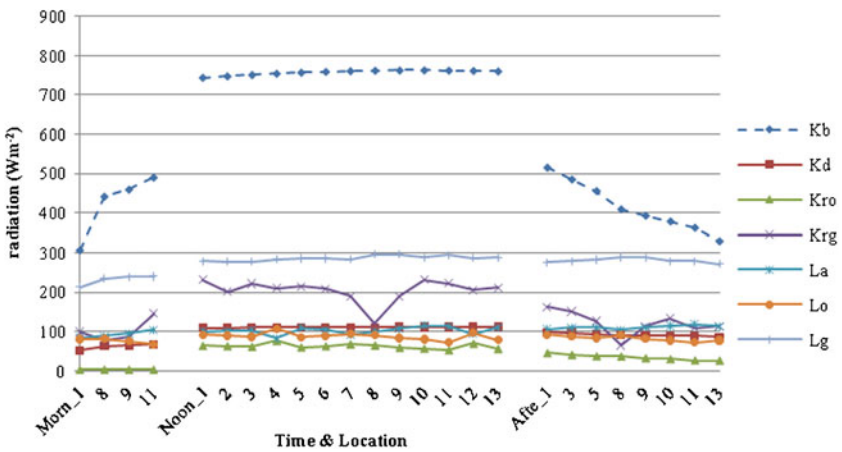

Fig. 2 Observed incoming solar and longwave radiation incident on a horizontal surface

Table 1 Collected climatic and radiation data on August 10, 2002 in Guelph, Ontario, Canada

Time	Site	Sky view factor (ψ_{sky})	Air temperature (T_a, °C)	Relative humidity (RH)	Solar altitude (β, °)	Radiation (W m^{-2})						
						K_b	K_d	K_{ro}	K_{rg}	L_a	L_o	L_g
Morning	1	0.60	19.6	0.891	23.0	306.7	51.5	2.5[a]	98.8	84.3	80.4	213.2
	8	0.60	21.3	0.741	31.7	441.8	63.4	3.0[a]	77.7	88.3	81.7	234.4
	9	0.64	21.7	0.721	32.8	459.6	64.8	3.0[a]	87.9	95.1	74.9	238.8
	11	0.68	22.6	0.680	34.9	490.4	67.1	2.9[a]	145.8	104.6	66.9	240.0
Noon	1	0.60	29.5	0.413	60.1	744.1	109.3	64.5	232.1	99.6	91.9	278.7
	2	0.61	29.4	0.408	60.6	747.8	109.6	63.3	201.2	101.4	89.4	277.4
	3	0.62	28.9	0.404	60.9	751.2	109.8	62.1	221.9	102.1	86.7	277.8
	4	0.53	28.5	0.398	61.3	754.5	110.1	76.8	210.2	82.6	107.6	283.9
	5	0.63	30.6	0.393	61.6	757.2	110.3	60.5	214.3	108.9	85.7	285.9
	6	0.62	29.9	0.387	61.9	759.4	110.5	63.3	208.6	103.8	88.7	286.2
	7	0.59	28.1	0.382	62.0	761.0	110.6	68.4	190.2	93.2	93.9	283.5
	8	0.60	29.3	0.377	62.3	762.1	110.8	65.6	121.9	99.7	91.0	296.0
	9	0.64	29.7	0.371	62.3	762.7	110.8	60.1	190.0	107.7	83.4	296.1
	10	0.66	31.3	0.366	62.4	762.9	110.9	57.3	231.3	115.6	80.9	287.8
	11	0.68	28.8	0.360	62.3	762.4	110.9	53.3	222.4	113.9	72.6	294.5
	12	0.58	29.1	0.354	62.3	761.6	110.9	70.0	204.8	93.5	97.3	287.2
	13	0.66	29.1	0.349	62.1	760.2	110.9	57.0	211.7	109.9	78.4	288.0
Afternoon	1	0.60	29.2	0.362	41.7	515.5	97.6	45.7	162.0	104.9	91.5	275.8
	3	0.62	29.7	0.365	39.6	485.6	95.9	41.3	151.4	110.0	87.6	279.0
	5	0.63	28.6	0.368	37.7	456.0	94.1	37.8	126.4	109.8	83.4	282.8
	8	0.60	28.7	0.374	34.7	409.7	91.2	36.8	64.9	104.3	90.3	289.0
	9	0.64	28.4	0.376	33.6	393.4	90.2	32.5	112.8	110.4	82.0	287.8
	10	0.66	28.4	0.377	32.8	379.1	89.3	30.0	133.5	113.9	77.9	278.6
	11	0.68	28.4	0.379	31.7	362.9	88.3	26.9	109.6	118.8	72.3	279.0
	13	0.66	28.3	0.383	29.7	329.9	86.1	26.4	113.4	113.8	77.6	272.0

[a] The low values of K_{ro} in the morning resulted from no reflection of direct beam solar radiation by the building surface which was shaded

radiation with sky view factors were used in the solar radiation calculation of all models:

$$K_d \rightarrow K_d \cdot \psi_{sky} \tag{17}$$

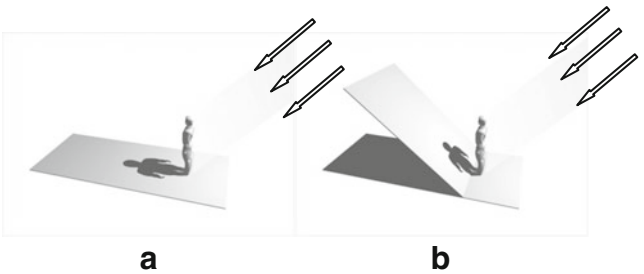

Fig. 3 Two different approaches to obtain projected areas: **a** shadow area on the horizontal ground surface (Burt and COMFA models), **b** shadow area on the surface perpendicular to sun's rays (RayMan, OUT_SET* and Park and Tuller model) (created using VectorWorks 2008)

$$(K_b + K_d)a_g \rightarrow \left(K_b \cdot \cos Z_{sl} \cdot t + K_d \cdot \psi_{w\_sky}\right)a_o + \left(K_b \cdot t + K_d \cdot \psi_{sky} + K_{ro}\right)a_g = K_{ro} + K_{rg} = K_r \tag{18}$$

The quantities of absorbed solar and net longwave radiation on the body surface area were compared among the models. The differences among them would be caused by their different adopted concepts of body shapes which resulted in various body area factors. They also use different methods of determining longwave radiation from the clear sky.

3 Results and discussion

3.1 Comparison of projected area factors (f_p^*)

Variations in the key factor in the analysis of direct beam solar radiation among models, f_p^*, are presented in Fig. 4.

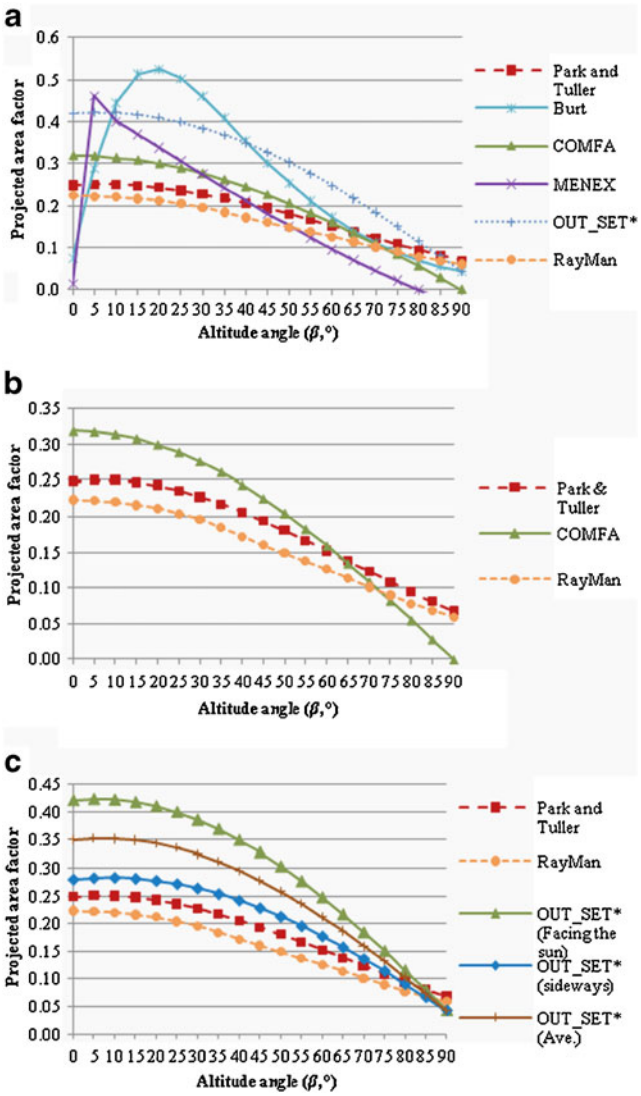

Fig. 4 Various comparisons of projected area factors (f_p^*). **a** Comparison of projected area factors (f_p^*), **b** comparison of f_p^* of Park and Tuller, RayMan and COMFA models and **c** comparison of f_p^* of Park and Tuller, RayMan and OUT_SET*

The horizontal shadow areas used in the Burt, COMFA and MENEX models were multiplied by sinβ to convert them to surface areas perpendicular to the sun's rays, equivalent to the projected area factors used in the other models.

The differences in f_p^* between the Park and Tuller model and Fanger's results used in the RayMan model are small, around 0.03 when β is less than 65°, and decrease as β approaches 90° (Fig. 4a). Next closest results to the Park and Tuller model were from the COMFA model which used a cylindrical body model. The maximum difference between them was 0.07 at β=0°. The difference decreased continually until β=63° and increased again up to 0.068 at β=90° (Fig. 4b). The OUT_SET* model used the results of Underwood and Ward's (1966) photographic method, but only considered the anterior/posterior of the body facing the sun, not the body sides (see Kerslake 1972). This overestimated f_p^* compared with a body exposed to the sun from a variety of directions. This creates more differences with the other photographic methods such as the Park and Tuller and RayMan models (Fig. 4c). The MENEX and Burt models had the highest values at β=5° and 20°, respectively, and crossing points with the Park and Tuller model around β=42° and 65°. Differences between f_p^* are greatest at low solar altitudes (Fig. 4a).

3.2 Absorbed radiation comparison

All five radiation estimating models and one experimental model, the six-directional method, were compared with the Park and Tuller model in absorbed solar, net longwave and net all-wave radiation because the Park and Tuller model was recently developed from a larger sample of people than previous studies (Park and Tuller 2010), and its results were close to the median of a group of models whose results were relatively close, i.e. six-directional method, COMFA, RayMan and Park and Tuller (Fig. 6).

3.2.1 Absorbed direct beam solar radiation (K_b^*)

In this study, β was 23.0–35.9° in the morning (0734–0845 hours), 60.1–62.4° around noon (1133–1244 hours) and 41.7–29.7° in the afternoon (1533–1642 hours).

Four of the six models (Park and Tuller, RayMan, COMFA and MENEX) form a group where values of absorbed direct beam solar radiation (K_b^*) are all relatively close, within 50 Wm^{-2} (Fig. 5). The Burt and OUT_SET* model results were above those of this model group. The Burt model deviated in the morning and afternoon and the OUT_SET* model at all times of the day. This mirrors the patterns of the projected area factor f_p^*. The Terjung and Louie (1971) method used in the Burt model had the highest f_p^* values of all models. This occurred at solar altitudes around 20°. Thus, the Burt model deviates from other models in f_p^* and K_b^* at times and observation sites

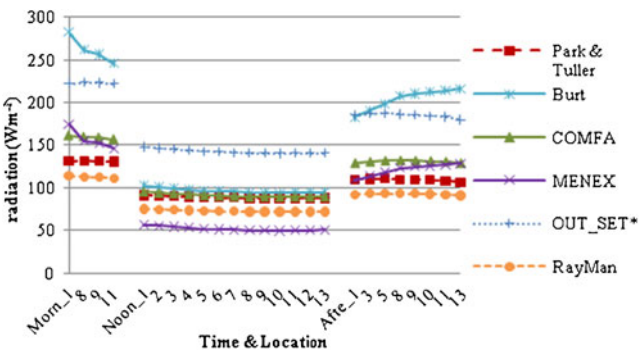

Fig. 5 Comparison of absorbed direct beam solar radiation on the body surface in the morning, around noon and in the afternoon

with solar altitudes near this value (Figs. 4 and 5). Its estimated K_b^* was up to 151 Wm^{-2} greater than that of the Park and Tuller model in the morning. The OUT_SET* model had a relatively high f_p^* value compared with most other models at all solar altitudes less than 80°. The MENEX model was within the group in the morning and afternoon except for station 1 in the morning (Morn_1) and had a difference of only around 30 Wm^{-2} with the group's median around noon (Fig. 5).

The closest results with the Park and Tuller model's were those of the RayMan model which had values that were 15–20 Wm^{-2} lower in the morning and afternoon and 16 Wm^{-2} lower around noon (Fig. 5). COMFA model results were very close to those of the Park and Tuller model around noon, within 1–4 Wm^{-2}.

3.2.2 Absorbed total solar radiation (R)

The OUT_SET* model had the greatest quantity of absorbed total solar radiation among all models for the day as a whole (Fig. 6a). It has a relatively high projected area factor and direct beam solar radiation as noted above. It is one of the models where diffuse beam and reflected solar radiation measured on a horizontal surface were not reduced by one half, producing greater quantities of these two radiation streams than most of the other models.

The MENEX model also had relatively high values of absorbed total solar radiation throughout the day (Fig. 6a). Its estimated direct beam solar radiation is close to that of most other models during the morning and afternoon and the lowest of all models at noon (Fig. 5). However, it differs from most other models in the lack of the ½ function correction for diffuse sources of radiation on/from a horizontal surface used as input in this study. It also does not apply an effective radiation area factor (f_{eff}) to these diffuse sources of radiation. These two factors combine to give the MENEX model the greatest diffuse beam and reflected solar radiation absorbed on the human body surface (Fig. 6d). The current version of MENEX has reduced the importance of diffuse radiation (http://www.igipz.pan.pl/geoekoklimat/blaz/MENEX_2005.pdf).

The COMFA model had the closest values to the Park and Tuller model around noon, about 4 Wm^{-2} differences. It had 14–27 Wm^{-2} more absorbed total solar radiation in the morning and afternoon. The Burt model also had close values to those of the Park and Tuller model around noon but had high values in the morning and afternoon close to those of the MENEX model because of its high f_p^* values. The six-directional method continually yielded 8–44 Wm^{-2} more than the Park and Tuller model's values. The RayMan model has a similar f_p ($=A_p/A_{eff}$) as the Park and Tuller model, but f_{eff} of the Park and Tuller model is 0.836 which is higher than RayMan's 0.725. Therefore, the RayMan f_p^*

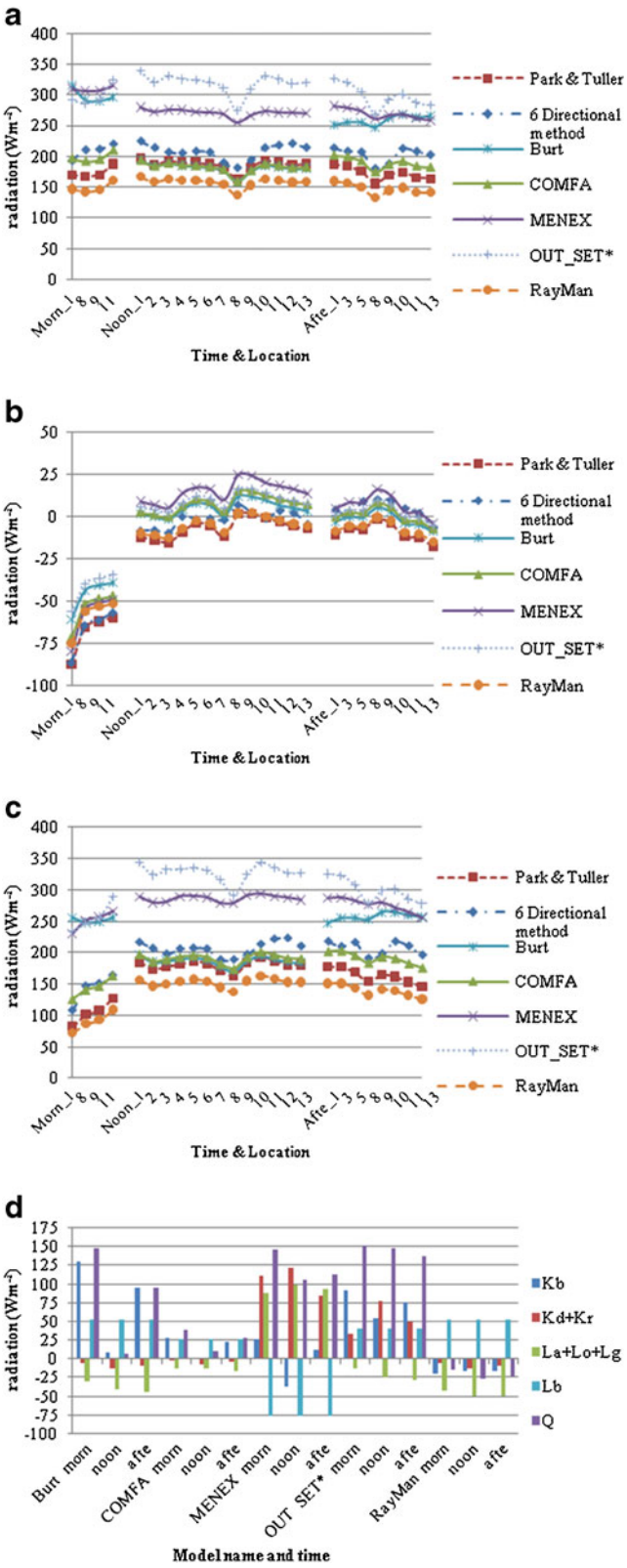

Fig. 6 Comparison of **a** absorbed total solar radiation, **b** net longwave radiation, **c** net all-wave radiation and **d** differences in absorbed and emitted radiation between the Park and Tuller model and the other models

($=A_p/A_D=f_p\times f_{eff}$) values were around 0.03 lower all day than the Park and Tuller model's. The lower RayMan f_p^* and f_{eff} values created somewhat lower absorbed direct beam, diffuse beam and reflected solar radiation than the Park and Tuller model's (Fig. 6d). Therefore, its absorbed total solar radiation was 23–30 Wm^{-2} lower.

3.2.3 Net longwave radiation (L)

The range between model estimates of net longwave radiation was not great, 31 Wm^{-2} between the OUT_SET* and Park and Tuller models in the morning and 23 Wm^{-2} between the MENEX and Park and Tuller models around noon and in the afternoon (Fig. 6b). The effective radiation area factor (f_{eff}) values and methods determining incoming longwave radiation from the open sky were the variables creating differences between models in this study. Differences in employed f_{eff} affect both the gain of absorbed and the loss of emitted longwave radiation. One offsets the other. The difference in net longwave radiation between models with unequal f_{eff} values will depend on the difference between incoming and emitted longwave radiation. The differences between these two radiation streams were not great in the very warm, sunny and summer conditions during our observations. The maximum daily mean difference in open sky longwave radiation (L_a) between models was only 19 Wm^{-2} (Fig. 7). These two factors combined to limit the magnitude of net longwave radiation differences between models.

Computed open sky incoming longwave radiation exceeded the measured value for all models that employed the computed values, OUT_SET*, COMFA, Burt and MENEX (Fig. 6b). The OUT_SET* model's method gave the greatest values. This combined with its relatively low f_{eff} (0.75) which limited the magnitude of the negative net longwave radiation gave it the greatest values during the morning. A high f_{eff} (1.0) and relatively high computed incoming sky longwave radiation gave the MENEX model

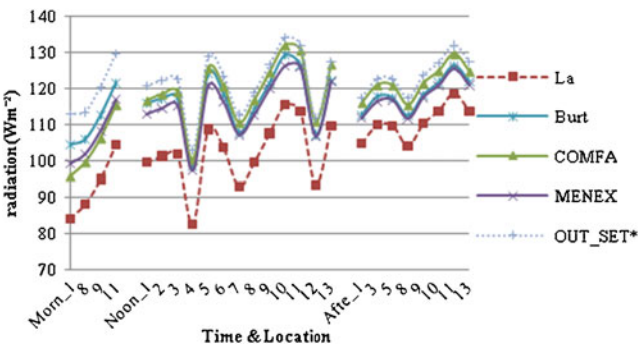

Fig. 7 Comparison between measured incoming longwave radiation from the open sky to the horizontal ground surface (L_a) and computed L_a results from the Burt, COMFA, MENEX and OUT_SET* models

the highest values during mid-day and the afternoon. The Park and Tuller model used the lower measured open sky longwave radiation values. Its relatively high f_{eff} accentuated the magnitude of its negative net longwave radiation, and it had the lowest net longwave radiation throughout the day (Fig. 6b). The values of the Park and Tuller and RayMan models were nearly identical near noon and in the afternoon.

3.2.4 Net all-wave radiation (Q)

Most of the variations in net all-wave radiation between models resulted from absorbed solar radiation. The greatest difference overall between the Park and Tuller model and the other models in net all-wave radiation was with the OUT_SET* model (Fig. 6c). The mean difference over the entire day was +146 Wm^{-2}, composed of the OUT_SET* model's 128 and 18 Wm^{-2} greater absorbed total solar and net longwave radiation, respectively (Fig. 6a, b). The second greatest difference was a 122 Wm^{-2} greater mean for the MENEX model. MENEX and OUT_SET* were the two models with the greatest absorbed total solar radiation for the day as a whole. The MENEX model also had the greatest net longwave radiation. The six-directional method had 36 Wm^{-2} greater net all-wave radiation than the Park and Tuller model, 29 and 7 Wm^{-2} more absorbed total solar and net longwave radiation, respectively.

The COMFA model had close results with the Park and Tuller model around noon. This model had larger differences at the lower solar altitudes (39, 10 and 27 Wm^{-2} in the morning, noon and afternoon). The RayMan model had the opposite phenomenon to the COMFA model. Its net all-wave radiation difference with the Park and Tuller model was relatively constant throughout the day, 15, 27 and 23 Wm^{-2} lower in the morning, noon and afternoon with the greater differences coming at the higher solar altitudes. The Burt model had the closest results with the Park and Tuller model around noon, but much larger differences in the morning (+147 Wm^{-2}) and afternoon (+94 Wm^{-2}) due to the greater gaps in absorbed direct beam solar radiation. Mean differences by time presented above between the Park and Tuller model and the other models are shown in Fig. 6d.

3.3 Correlation among the models

Pearson's product–moment correlation coefficients between models were determined for absorbed total solar, net longwave and net all-wave radiation (Tables 2 and 3). The inputs were the 25 time–site values from the models.

Time and site differences in longwave radiation were determined by the variations in measured quantities of longwave radiation, air temperature and humidity depend-

Table 2 The correlation among the models for absorbed total shortwave (top half) and net longwave (bottom half) radiation

	Shortwave						
Longwave	Park and Tuller model	6-directional method	COMFA model	MENEX model	Burt model	RayMan model	OUT_SET* model
Park and Tuller model		0.652[a]	0.320	0.105	−0.537	0.996[a]	0.994[a]
6-directional method	0.983[a]		0.587[a]	0.344	−0.011	0.683[a]	0.684[a]
COMFA model	0.996[a]	0.967[a]		0.742[a]	0.621[a]	0.401	0.400
MENEX model	0.995[a]	0.966[a]	1[a]		0.593[a]	0.161	0.126
Burt model	0.993[a]	0.959[a]	0.999[a]	0.999[a]		−0.459	−0.466
RayMan model	1[a]	0.983[a]	0.996[a]	0.995[a]	0.993[a]		0.997[a]
OUT_SET* model	0.993[a]	0.958[a]	0.999[a]	0.999[a]	1[a]	0.993[a]	

[a] Correlation coefficient (r) is significant at the 0.01 level (two-tailed)

ing on the model. The major control of differences in the computed open sky incoming longwave radiation was air temperature. The time–site correlation between air temperature and the measured amount of incoming longwave radiation from the upper hemisphere was 0.963. Hence, the time–site variations in longwave radiation were similar for all models producing very significant correlations in human body net longwave radiation, all over 0.95 and many over 0.99 (Table 2).

Correlations for absorbed total solar radiation were determined mainly by variation patterns of the projected area factor (f_p^*) with solar altitude. Models whose graphs of f_p^* with solar altitude have similar shape through the range of solar altitudes encountered in the field observations (23° to 63°) will have high correlation coefficients (Fig. 4, Table 2). Those whose shapes differ will have low correlations. Correlation coefficients between the Park and Tuller, RayMan and OUT_SET* models were all very significant (over 0.994). The Burt and MENEX models whose curves have unique shapes have the lowest correlations with other models.

The correlations for net all-wave radiation were also very significant among the Park and Tuller, RayMan and OUT_SET* models even though all models except the Burt model had correlations over 0.90 (Table 3). Only these three models had high correlations for both absorbed total solar and net longwave radiation. The strongest correlation was between the Park and Tuller and RayMan models, r= 0.999, as expected. The correlations between the Park and Tuller and OUT_SET* models and between the RayMan and OUT_SET* models were r=0.953 and r=0.947, respectively (Table 3).

4 Conclusions

The radiation components of five existing human thermal exchange models (Burt, COMFA, MENEX, OUT_SET* and RayMan models), one experimental model [six-directional method from VDI (1998)] and the new Park and Tuller model were compared.

Results of all models were referenced against those of the Park and Tuller model. This is not to suggest this model is the most appropriate for all applications. It is the one that employs the most recently derived human body radiation area factors. It puts the comparisons in the time perspective.

Table 3 The correlation among the models for net all-wave radiation

Net all-wave radiation	Park and Tuller model	6-directional method	COMFA model	MENEX model	Burt model	RayMan model	OUT_SET* model
Park and Tuller model	1						
6-directional method	0.911[a]	1					
COMFA model	0.957[a]	0.948[a]	1				
MENEX model	0.951[a]	0.836[a]	0.912[a]	1			
Burt model	−0.593[a]	−0.326	−0.336	−0.583[a]	1		
RayMan model	0.999[a]	0.919[a]	0.964[a]	0.947[a]	−0.569[a]	1	
OUT_SET* model	0.953[a]	0.825[a]	0.889[a]	0.928[a]	−0.641[a]	0.947[a]	1

[a] Correlation coefficient (r) is significant at the 0.01 level (two-tailed)

Direct comparison with this model eases the identification of differences that might arise when using older, widely employed or more recent methods. The Park and Tuller radiation area factors were developed from a larger sample of actual adults and used up-to-date video and computer technology compared with most of the older methods. However, it has not undergone the testing of extensive applications experienced by the older methods.

Absolute net longwave radiation differences between models were not great (maximum difference, 31 Wm^{-2}). Although effective radiation area factors (f_{eff}) had a wide range from 0.725 to 1.0, the magnitude of the differences between human body absorbed and emitted longwave radiation was also relatively small. This and the limited range between incoming longwave radiation from the sky used in the models (measured and computed) limited the magnitude of model differences in net longwave radiation. The situation can be different at other times and in other environments, e.g. very cold or hot radiant environments where environmental radiant temperature differs markedly from human surface/clothing temperature. In these types of environments, inappropriate f_{eff} values can lead to larger errors in estimated human net longwave radiation.

All four methods of computing incoming longwave radiation from the clear sky overestimated the measured value. The Idso (1981) method used in the OUT_SET* model yielded the highest value followed by the Swinbank (1963) equation (COMFA), Brunt (1932) method (Burt model) and that found in Geiger (1965) used by MENEX. However, the differences between computation methods were small, 7.5 Wm^{-2} for the day as a whole. The variation between the mean from all four computation methods and measured open sky longwave radiation was 14 Wm^{-2}. Measured longwave radiation data are seldom available, and estimates must be made for many applied climate studies. In most cases, the differences we found between measured and computed open sky longwave radiation and between those estimated by different formulas will not have a major impact on human net all-wave or total thermal exchange evaluations.

A key variable in model absorbed solar radiation differences is the projected area factor (f_p^*). The empirical MENEX and Burt models' factors had a great deal of variation with solar altitude compared with the other models whose curves have a much lower slope (Fig. 4). Human body direct beam solar radiation estimated using these two models is more sensitive to variations in solar altitude. Moreover, the Burt model has a crossing point of its f_p^* line with Park and Tuller model's f_p^* line near the noon solar altitude in this study so that the model had results close to those of the Park and Tuller model at noon. However, the model can produce very different noon results at other seasons and latitudes that have different solar altitudes.

The OUT_SET* model's elliptical cylinder body model has higher f_p^* values than most of the other models at solar altitudes less than 80°. The major axis of the ellipse facing the sun maximizes the projected area factor compared with models that incorporate the sun's rays intersecting all sides of the body. E.g. OUT_SET*'s f_p^* is between 0.07 and 0.10 greater than that of the non-elliptical cylinder used in the COMFA model (Fig. 4). This creates relatively high absorbed direct beam and total solar radiation (Figs. 5 and 6).

The RayMan model has f_p^* values very similar to those of the Park and Tuller model, 0.035–0.025 lower, which produced about 27 Wm^{-2} lower absorbed total solar radiation during the daytime.

Both effective radiation area and whether or not diffuse sources of radiation measured on or from a horizontal surface are reduced by one half to account for a unit area of the vertical body surface's exposure to only half the entire horizontal surface were important controls of model differences in estimated human body diffuse beam and reflected-from-the-ground solar radiation. The MENEX model had the highest total of human diffuse beam and reflected solar radiation simply because of its implied 1.0 f_{eff} and no ½ function (Fig. 6d). The ½ function is quantitatively the more important than most differences in f_{eff}. Next highest was the OUT_SET* model which had a relatively low f_{eff} value of 0.75 but did not have the ½ function. Studies need to be very clear about the surfaces on which diffuse radiation components used as model input data are measured or estimated. The ½ function applies to input data on a horizontal surface but not to direct measurement or estimation on a vertical surface.

Human radiation exchange has widespread application and can aid in the planning of more comfortable and healthy environments for people. Several human radiation exchange models are available employing a variety of different assumptions. This study has compared a selection of these models. Several radiation streams were derived from measured data and were the same for all models. Therefore, model differences were created by the input of longwave radiation from the clear sky and human body projected area (f_p) and effective radiation area (f_{eff}) factors used in each model. Values of these human radiation area factors were determined via different methods including using samples of people or mannequins of different age, size and shape or objects such as cylinders. Model differences in human net all-wave radiation were up to about 150 Wm^{-2} which can have an important effect on thermal sensation.

It is suggested that those estimating human radiation exchange study a variety of models and take care to select

algorithms and human radiation area factors that are most applicable to the subjects of their study. We also encourage more direct comparison of available models in a variety of different environments. These types of studies will help those wishing to estimate human radiation exchange select appropriate models and methods.

References

Ali-Toudert F, Djenane M, Bensalem R, Mayer H (2005) Outdoor thermal comfort in the old desert city of Beni-Isguen, Algeria. Clim Res 28:243–256. doi:10.3354/cr028243

Blazejczyk K, Nilsson H, Holmér I (1993) Solar heat load on man: review of different methods of estimation. Int J Biometeorol 37:125–132. doi:10.1007/BF01212621

Blazejczyk K (1994) New climatological-and-physiological model of the human heat balance outdoor (MENEX) and its applications in bioclimatological studies in different scales. In: Blazejczyk K, Krawczyk B (ed) Bioclimatic research of the human heat balance. Polish Academy of Sciences, Institute of Geography and Spatial Organization, Warsaw, pp 27–58

Blazejczyk K (2004) Assessment of radiation balance in man in various meteorological and geographical conditions. Geogr Pol 77:63–76

Blazejczyk K (2005) MENEX_2005-the updated version of man-environment heat exchange model. http://www.igipz.pan.pl/geoekoklimat/blaz/MENEX_2005.pdf. Accessed 31 December 2010, 14 pp

Brown RD, Gillespie TJ (1986) Estimating outdoor thermal comfort using a cylindrical radiation thermometer and an energy budget model. Int J Biometeorol 30:43–52. doi:10.1007/BF02192058

Brown RD, Gillespie TJ (1995) Microclimatic landscape design: creating thermal comfort and energy efficiency. Wiley, New York

Brunt D (1932) Notes on radiation in the atmosphere. Q J R Meteorol Soc 58:389–420. doi:10.1002/qj.49705824704

Burt JE (1979) A model of human thermal comfort and associated comfort patterns for the United States. C. W. Thornthwaite Associates, Centerton

Fanger PO (1972) Thermal comfort: analysis and applications in environmental engineering. McGraw-Hill, New York

Gagge AP, Stolwijk JAJ, Nishi Y (1969) The prediction of thermal comfort when thermal equilibrium is maintained by sweating. ASHRAE Trans Part 2:108–123

Geiger R (1965) The climate near the ground. Havard University Press, Cambridge

Guibert A, Taylor CL (1952) Radiation area of the human body. J Appl Physiol 5:24–37

Huang H, Ooka R, Kato S (2005) Urban thermal environment measurements and numerical simulation for an actual complex urban area covering a large district heating and cooling system in summer. Atmos Environ 39:6362–6375. doi:10.1016/j.atmosenv.2005.07.018

Idso SB (1981) A set of equations for full spectrum and 8- to 14-micrometre and 10.5- to 12.5-micrometre thermal radiation from cloudless skies. Water Resour Res 17:295–304

Iziomon MG, Mayer H, Matzarakis A (2003) Downward atmospheric longwave irradiance under clear and cloudy skies: measurement and parameterization. J Atmos Sol Terr Phys 65:1107–1116. doi:10.1016/j.jastp.2003.07.007

Jendritzky G, Nübler W (1981) A model analyzing the urban thermal environment in physiologically significant terms. Arch Meteor Geophy B 29:313–326

Jendritzky G, Menz H, Schirmer H, Schmidt-Kessen W (1990) Methodik zur raumbezogenen Bewertung der thermischen Komponente im Bioklima des Menschen (Fortgeschriebenes Klima-Michel-Modell). Beitr Akad Raumforsch Landesplan, No. 114

Kenny NA, Warland JS, Brown RD, Gillespie TG (2008) Estimating the radiation absorbed by a human. Int J Biometeorol 52:491–503. doi:10.1007/s00484-008-0145-8

Kerslake DM (1972) The stress of hot environments. Cambridge University Press, Cambridge. ISBN 0-521-08343-5

Krys SA, Brown RD (1990) Radiation absorbed by a vertical cylinder in complex outdoor environment under clear sky conditions. Int J Biometeorol 34:69–75. doi:10.1007/BF01093450

Kubaha K, Fiala D, Toftum J, Taki AH (2004) Human projected area factors for detailed direct and diffuse solar radiation analysis. Int J Biometeorol 49:113–129. doi:10.1007/s00484-004-0214-6

Matzarakis A, Rutz F, Mayer H (2000) Estimation and calculation of the mean radiant temperature within urban structures. In: de Dear RJ, Kalma JD, Oke TR, Auliciems A (ed) Biometeorology and urban climatology at the turn of the millennium. ICB-ICUC'99, Sydney, WCASP-50, WMO/TD No 1026, 273-278

Matzarakis A, Rutz F, Mayer H (2007) Modelling radiation fluxes in simple and complex environments-application of the RayMan model. Int J Biometeorol 51:323–334. doi:10.1007/s00484-006-0061-8

Matzarakis A, Rutz F, Mayer H (2009) Modelling radiation fluxes in simple and complex environments: basics of the RayMan model. Int J Biometeorol 54:131–139. doi:10.1007/s00484-009-0261-0

Oliveira S, Andrade H (2007) An initial assessment of the bioclimatic comfort in an outdoor public space in Lisbon. Int J Biometeorol 52:69–84. doi:10.1007/s00484-007-0100-0

Park S (2003) Estimating radiation received by a person in the landscape. MSc thesis, University of Guelph

Park S, Tuller SE (2010) Human body area factors for radiation exchange analysis: Standing and Walking postures. Int J Biometeorol (published online). doi:10.1007/s00484-010-0385-2

Parsons K (1993) Human thermal environments: the effects of hot, moderate and cold environments on human health, comfort and performance-the principles and the practice. Taylor & Francis, London

Pickup J, de Dear R (2000) An outdoor thermal comfort index (OUT-SET*)—part I—the model and its assumptions. In: de Dear R, Kalma J, Oke T, Auliciems A (ed) Biometeorology and urban climatology at the turn of the millennium-selected papers from the conference ICB-ICUC'99 (Sydney, 8–12 November 1999), WCASP-50, WMO/TD-No. 1026. World Meteorological Organization, Geneva, pp 279–283

Spagnolo J, de Dear R (2003) A field study of thermal comfort in outdoor and semi-outdoor environments in subtropical Sydney Australia. Build Environ 38:721–738. doi:10.1016/S0360-1323(02)00209-3

Steadman RG (1971) Indices of windchill of clothed persons. J Appl Meteorol 10:674–683. doi:10.1175/1520-0450(1971)010<0674:IOWOCP>2.0.CO;2

Steadman RG (1979) The assessment of sultriness. Part II: effects of wind, extra radiation and barometric pressure on apparent temperature. J Appl Meteorol 18:874–885. doi:10.1175/1520-0450(1979)018<0874:TAOSPI>2.0.CO;2

Swinbank WC (1963) Long-wave radiation from clear skies. Q J R Meteorol Soc 89:339–348. doi:10.1002/qj.49708938105

Tanabe S, Narita C, Ozeki Y, Konishi M (2000) Effective radiation area of human body calculated by a numerical simulation. Energ Buildings 32:205–215. doi:10.1016/S0378-7788(00)00045-1

Terjung WH, Louie S (1971) Potential solar radiation climates of man. Ann Assoc Am Geogr 61:481–500. doi:10.1111/j.1467-306.1971.tb00801.x

Thorsson S, Lindberg F, Eliasson I, Holmer B (2007) Different methods for estimating the mean radiant temperature in an outdoor urban setting. Int J Climatol 27:1983–1993. doi:10.1002/joc.1537

Tuller SE (1990) Standard seasons. Int J Biometeorol 34:181–188. doi:10.1007/BF01048718

Underwood CR, Ward EJ (1966) The solar radiation area of man. Ergonomics 9:155–168. doi:10.1080/00140136608964361

Ward EJ, Underwood CR (1967) Effect of posture on the solar radiation area of man. Ergonomics 10:399–409. doi:10.1080/00140136708930887

VDI (1998) VDI 3787, part 2: environmental meteorology-methods for the human biometeorological evaluation of climate and air quality for urban and regional planning at regional level part 1: climate. Beuth, Berlin